The Hubbard model on the triangular lattice: a slave-boson study

1997 J. Phys.: Condens. Matter 9 L27

(http://iopscience.iop.org/0953-8984/9/4/001)

INSTITUTE OF PHYSICS PUBLISHING JOURNAL OF PHYSICS: CONDENSED MATTER

J. Phys.: Condens. Matter **9** (1997) L27–L32 www.iop.org/Journals/cm PII: S0953-8984(97)78862-3

LETTER TO THE EDITOR

The Hubbard model on the triangular lattice: a slave-boson study

A Feiguin, C J Gazza, A E Trumper and H A Ceccatto

Instituto de Física Rosario, Consejo Nacional de Investigaciones Científicas y Técnicas and Universidad Nacional de Rosario, Boulevard 27 de Febrero 210 Bis, 2000 Rosario, Argentina

Received 22 October 1996

Abstract

We study the Hubbard model on the triangular lattice for general fillings by means of the slave-boson technique. In particular, we consider the stability regions of the paramagnetic, antiferromagnetic and linearly polarized spin-density-wave phases that are present at half-filling. The model presents a large anisotropy under particle or hole doping of the half-filled band, a consequence of the non-bipartite nature of the lattice. We also compute the helicity modulus in the antiferromagnetic phase, which characterizes the stiffness of the magnetic order.

The Hubbard model [1], the paradigm of the highly correlated electron systems, has been extensively studied in the last few years mainly because of its possible connections with the physics of the CuO_2 planes in high-T_c ceramic compounds. Because of this motivation, most authors have considered the behaviour of this model on the square lattice, particularly in the limit of large on-site Coulomb repulsion U. At half-filling this system is an antiferromagnetic insulator for all values of U, because of the perfect nesting of the non-interacting Fermi surface. Interesting features in the ground-state magnetic properties, like incommensurate spiral structures, appear only away from half-filling [2–4].

The Hubbard model for geometries other than the square lattice has received much less attention. However, its behaviour becomes more interesting when one considers, for instance, non-bipartite lattices. In particular, it has been shown [5–7] that on the triangular lattice even at half-filling it has a very rich ground-state structure, including a paramagnetic phase, different magnetic long-range orders, and a metal–insulator transition. All this physics has its origin in the combined effects of the large electron correlation and the magnetic frustration characteristic of the lattice.

In this work we consider the Hubbard model on the triangular lattice:

$$H = -t \sum_{i,\mu,\sigma} c^{\dagger}_{i\sigma} c_{i+\mu,\sigma} + U \sum_{i} n_{i\uparrow} n_{i\downarrow} \tag{1}$$

where i indicates lattice sites and the μs are the vectors pointing to the six nearest neighbours of a given site. This model has been studied in [5–7] using the Hartree–Fock (HF) approximation, and we have previously considered [8] its phase diagram at half-filling ($\delta \equiv 1 - n = 0$) by means of the slave-boson (SB) mean-field approach. In this work we extend our calculations

0953-8984/97/040027+06$30.00

away from half-filling, to explore the behaviour of the model in the absence of particle–hole symmetry due to the non-bipartite nature of the triangular lattice. Even though this study has already been performed using the Hartree–Fock approximation, the differences between the HF and SB results found for $n = 1$ [8] make the investigation worth pursuing. On the other hand, as shown in [9] for the Hubbard model on the square lattice, the SB technique greatly improves on HF results, especially away from half-filling.

In particular, we will consider the stability regions in the (δ, U) parameter space of the three phases found to be stable at half-filling in [8]: the paramagnetic (P), three-sublattice antiferromagnetic (AF), and linearly polarized spin-density-wave (LSDW) phases. We will not investigate the possibility of having spiral phases, which are suppressed at $\delta = 0$ with respect to the HF predictions by the lowering of the paramagnetic energy in the SB approach. We will also disregard, for the time being, the interesting questions of Nagaoka (ferromagnetic) instabilities and phase separation for large U [7], and the existence of vortex–lattice magnetic structures for particular fillings found in unrestricted HF calculations [10].

We use the rotationally invariant SB approach as developed in [11]. Although this formulation is not strictly necessary at the mean-field level, it is convenient for treating non-collinear phases. Following the notation in [8], in the P and AF phases the pseudofermion dispersion relations are given by

$$\epsilon_{k\sigma} = \frac{(A_{k\uparrow} + A_{k\downarrow})}{2} - \sigma\sqrt{\left(\frac{A_{k\uparrow} - A_{k\downarrow}}{2}\right)^2 + B_k^2} \qquad (\sigma = \pm). \tag{2}$$

We have used the definitions

$$A_{k\sigma} = t\alpha_\sigma^2\gamma_k^c + \lambda_0^{(2)} + \sigma\lambda_3^{(2)} \qquad B_k = t\gamma_k^s\alpha_\uparrow\alpha_\downarrow \tag{3}$$

with

$$\gamma_k^c = \frac{1}{2}\sum_{\mu,\sigma}\cos\left(k + \sigma\frac{Q}{2}\right)\cdot\mu \qquad \gamma_k^s = \frac{1}{2}\sum_{\mu,\sigma}\sigma\cos\left(k + \sigma\frac{Q}{2}\right)\cdot\mu. \tag{4}$$

In the P and AF phases the magnetic wavevector $Q = 0$, $(4\pi/3, 0)$ respectively, but (2)–(4) hold for an arbitrary spiral phase. The α_σs are the Kotliar–Ruckenstein [12] *ad hoc* factors

$$\alpha_\sigma = \frac{1}{\sqrt{1 - d^2 - p_\sigma^2}}(ep_\sigma + dp_{-\sigma})\frac{1}{\sqrt{1 - e^2 - p_{-\sigma}^2}}$$

which renormalize the bandwidth to ensure the correct $U = 0$ limit. Here e^2, $p_\uparrow^2$, $p_\downarrow^2$, and d^2 are, respectively, the probabilities of having a hole, a single electron (polarized parallel or antiparallel to the local z-axis), and double occupancy. Finally, in (3) $\lambda_0^{(2)}$ and $\lambda_3^{(2)}$ are the Lagrange multipliers that impose the equivalence in computing the mean particle and spin densities using either these probabilities or the pseudofermion densities.

Then, the ground-state energy of model (1) in the SB approach becomes

$$E_0 = H_0 + \sum_{k,\sigma}\epsilon_{k\sigma}n_{k\sigma} \tag{5}$$

where the $n_{k\sigma}$s are the pseudofermion occupation numbers. The constant

$$H_0 = Ud^2 - \lambda^{(1)}(e^2 + p_\uparrow^2 + p_\downarrow^2 + d^2 - 1) + \lambda_0^{(2)}(p_\uparrow^2 + p_\downarrow^2 + 2d^2) + \lambda_3^{(2)}(p_\uparrow^2 - p_\downarrow^2)$$

takes into account the Coulomb energy (the first term in the rhs) and includes the contributions of the averaged constraints. Notice the term with the $\lambda^{(1)}$-multiplier that restricts, on average, the bosonic sector of state space to the physical size (sites probabilities must add up to one). The minimization of (5) with respect to the Lagrange multipliers and site probabilities produces seven consistency equations that are solved numerically. Like in [8], we use an iterative method

that requires, at every step, adjusting the chemical potential μ to fix the particle density to $n = 1 - \delta$. To allow a precise determination of the Fermi surface, in the P phase we solve the problem using an 800×800 grid to cover the Brillouin zone (this large number of points is required to make the iterative procedure a stable minimization algorithm). In the gapped AF phase we used the Gauss–Legendre integration method with 120×120 points. We checked that these approximations produce no perceptible error in the curves shown below. Notice that for $\boldsymbol{Q} = \boldsymbol{0}$ one could have used the density of states obtained in [7] to evaluate the k-space integrals.

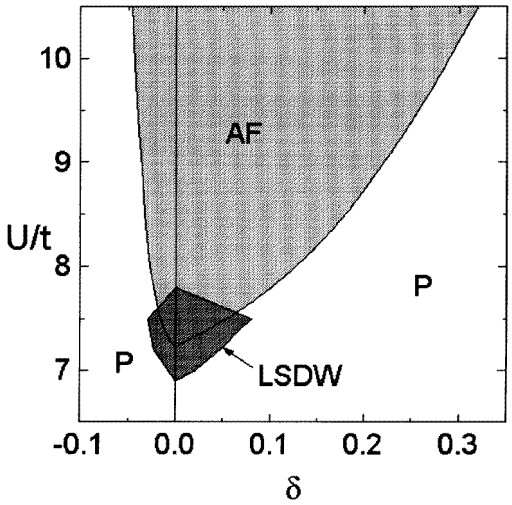

Figure 1. Stability regions in the (δ, U) parameter space of the paramagnetic (P), antiferromagnetic (AF), and linear spin-density-wave (LSDW) phases of the Hubbard model on the triangular lattice.

In figure 1 we present the result of the numerical procedure described above. This figure shows a large asymmetry in the stability of the AF phase under particle or hole doping from half-filling. For instance, for $U/t = 9$ the AF order is destroyed by $\sim$4% of additional particles, while it takes $\sim$22% of holes to produce the same effect. This asymmetric behaviour is even more pronounced for larger values of U. In figure 2 we give the dispersion relations (2) in the AF phase for $U/t = 9$ and different δ-values, along the following path in the Brillouin zone:

$$\Gamma = (0, 0) \rightarrow \mathrm{X} = (\pi, \pi/\sqrt{3}) \rightarrow \mathrm{W} = (2\pi/3, 2\pi/\sqrt{3}) \rightarrow \mathrm{Z} = (0, 2\pi/\sqrt{3}). \tag{6}$$

This figure shows the behaviour of the bands at half-filling and for doping values that are intermediate and close to the P phase transition. As can be seen, there is a sizable band renormalization and a diminishing gap for increasing doping with respect to half-filling. At the point where the P phase becomes stable there is still a finite local magnetization, which indicates that the predicted AF–P transition is of first order. Moreover, the itinerant magnetic state rapidly loses energy with the disordered state when the spin-down quasiparticle excitations begin to be populated.

At half-filling there is a commensurate LSDW state [6], which competes with the P and AF phases in a small range $6.9 \leqslant U/t \leqslant 7.8$. This state becomes favourable against the AF order because of the zigzagging ferromagnetic pathways that it presents (see figure 3), which lower the kinetic energy to the point of overcoming the loss in magnetic energy. Conversely, it is stable against the disordered state because of its gain in magnetic energy. Studying this order

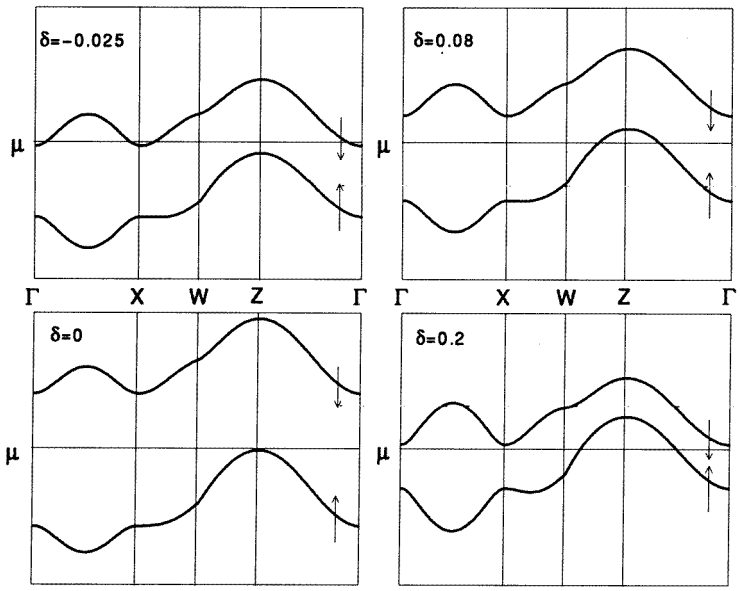

Figure 2. Quasiparticle energy bands along the Γ–X–W–Z path in the Brillouin zone (given in (6) in the main text), for $U/t = 9$ and different fillings.

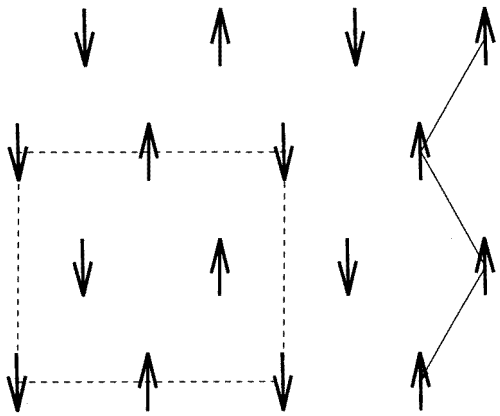

Figure 3. The magnetization pattern in the commensurate LSDW state. The dashed line shows the four-site unit cell. Notice the zigzagging ferromagnetic pathways.

away from half-filling requires considerable numerical effort, since the dispersion relations cannot be obtained analytically because of the enlargement of the magnetic cell. Like in our previous study [8] for $\delta = 0$, we solved the corresponding consistency equations on a grid of 200×200 points covering the Brillouin zone of the new decorated rectangular lattice. As shown in figure 1, the LSDW phase is stable in a small region, with a pronounced asymmetric shape.

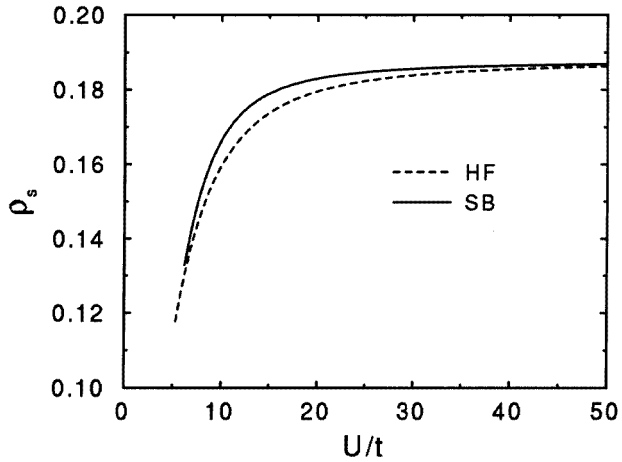

Figure 4. The helicity modulus ρ_s at half-filling in the AF phase. Full and dashed lines are the SB and HF results respectively.

We have also computed the helicity modulus or spin stiffness in the AF phase at half-filling:

$$\rho_s = \lim_{q\to 0} \frac{E_0(q) - E_0(0)}{\frac{1}{2}q^2}$$

with $E_0(q)$ obtained by taking $\boldsymbol{Q} = (4\pi/3 - q, 0)$ in (4). This important quantity in the study of quantum systems measures the stiffness of the ordered state under a twist in the order parameter. In this particular case it gives the rigidity of the AF state to small changes in the spiral wavevector. By following the calculations in [9] we obtained the result shown in figure 4. We also present in this figure the corresponding result obtained using the HF approximation. As concluded in [9], in both cases the helicity modulus is essentially determined by the average kinetic energy. However, by comparison with Monte Carlo results, Denteneer and Blaauboer showed that for the square lattice the SB results improve on those of the HF approximation. We believe that this should also happen on the triangular lattice. In any case, like on the square lattice, the HF and SB predictions for ρ_s do not differ much.

In conclusion, we have studied the Hubbard model on the triangular lattice for general fillings by means of the SB technique. Our results show a large asymmetry in the behaviour of the system around half-filling under particle or hole doping, a consequence of the non-bipartite nature of the lattice. In particular, for $t > 0$ in (1), particles are much more efficient than holes in destroying the AF order. Since we are not considering boson fluctuations, our approach is expected to overestimate the robustness of the AF state. The relatively small particle doping required to destroy this order makes it tempting to speculate that antiferromagnetism could be a sort of critical state at half-filling, with perhaps a ground-state structure closer to Anderson's resonant-valence-bond ideas for very small $\delta < 0$. With hole doping, however, the antiferromagnetic order seems to be fairly robust. The SB approach predicts a first-order transition between the AF and P phases, while the LSDW phase remains the stable ground-state structure in a small parameter region. We have also computed the helicity modulus (or spin stiffness) of the system at half-filling in the AF phase, which, like for the square lattice, does not differ much from the HF prediction.

References

[1] Hubbard J 1963 *Proc. R. Soc.* A **276** 238
Hubbard J 1964 *Proc. R. Soc.* A **281** 401
[2] Shraiman B I and Siggia E D 1989 *Phys. Rev. Lett.* **62** 1564
[3] Schultz H J 1990 *Phys. Rev. Lett.* **64** 1445
[4] Frésard R, Dzierzawa M and Wolfle P 1991 *Europhys. Lett.* **15** 325
[5] Krishnamurthy H R, Jayaprakash C, Sarker S and Wenzel W 1990 *Phys. Rev. Lett.* **64** 950
[6] Jayaprakash C, Krishnamurthy H R, Sarker S and Wenzel W 1991 *Europhys. Lett.* **15** 625
[7] Hanisch T, Kleine B, Ritzl A and Muller-Hartmann 1995 *Ann. Phys., Lpz.* **4** 303
[8] Gazza C J, Trumper A E and Ceccatto H A 1994 *J. Phys.: Condens. Matter* **6** L625
[9] Denteneer P J H and Blaauboer M 1995 *J. Phys.: Condens. Matter* **7** 151
[10] Fujita M, Nakanishi T and Machida K 1992 *Phys. Rev.* B **45** 2190
[11] Li T, Wolfle P and Hirschfeld P J 1989 *Phys. Rev.* B **40** 6817
[12] Kotliar G and Ruckenstein A E 1986 *Phys. Rev. Lett.* **57** 1362